 doi:10.20944/preprints202210.0087.v1

Article

Molecular Characterization of the Stress Response of the Holothurian Central Nervous System

Sebastián Cruz-González[1], Eduardo Quesada-Díaz[1], Yamil Miranda-Negrón[1], Raúl García-Rosario[1], Humberto Ortiz-Zuazaga[2], José E. García-Arrarás[1]

[1]Department of Biology, College of Natural Sciences, University of Puerto Rico, Río Piedras, Puerto Rico; [2]Department of Computer Science, College of Natural Sciences, University of Puerto Rico, Río Piedras, Puerto Rico

Abstract: Injury to the central nervous system (CNS), in most vertebrate animals, results in permanent damage and lack of function, due to their limited regenerative capacities. In contrast, echinoderms can fully regenerate their radial nerve cord (RNC) following transection, with little or no scarring. Investigators have associated the regenerative capacity of some organisms to the stress response and inflammation produced by the injury. Here we explore the gene activation profile of the stressed holothurian CNS. To do this, we performed RNA sequencing on isolated RNC explants submitted to the stress of transection and enzyme dissection and compared to explants kept in culture for 3 days following dissection. We describe stress-associated genes, including members of heat-shock families, ubiquitin-related pathways, transposons and apoptosis that were differentially expressed. Surprisingly, the stress response does not induce apoptosis in this system. Other genes associated with stress in other animal models, such as hero proteins and those associated with the integrated stress response, were not found to be differentially expressed either. Our results provide a new viewpoint on the stress response in the nervous system of an organism with an amazing regenerative capacity. This is the first step to decipher the molecular processes that allow echinoderms to undergo fully functional CNS regeneration while also providing a comparative view for students of the stress response in other organisms.

Keywords: Echinoderm; heat shock proteins; ubiquitin; regeneration; RNA-seq; spinal cord injury

Introduction

In higher vertebrates, such as humans, severe trauma to their Central Nervous System (CNS) can lead to life-long paralysis, while less complex organisms are capable of extensive CNS regeneration [1]. The reason behind such significant differences in regenerative potential remains unclear. However, recent studies have pinpointed the initial stress response to CNS trauma as a trigger of subsequent events that may limit overall tissue regeneration [2]. Paradoxically, the very mechanisms by which the CNS in higher vertebrates responds to damage leads to its regenerative incompetence. At the cellular and transcriptomic level, past research has often divided the response to spinal cord injury (SCI), a common CNS lesion, into an acute phase (~24 hrs), a subacute phase (2-7 days), and a chronic phase (weeks, months) [3][4][5][6][7]. The acute phase corresponds to the direct effect of the injury on the tissue, while both the subacute and the chronic phases are mediated mainly by the immune system or other events that originate from the acute response. The early response to trauma is of particular note; it is essential for wound healing and clearing of debris at the injury site but, if prolonged and excessive, it leads to secondary damage such as glial scarring. This scarring creates a milieu unfavorable for tissue renewal [8]. Experiments in non-mammalian species, particularly fishes and amphibians, have shown some peculiarities that may account for the increased regenerative potential of these species [9][10][11][12][13]. Thus, investigators have probed the gene expression profiles of species that can regenerate their spinal cord, following transection, as a source

 doi:10.20944/preprints202210.0087.v1

of insights (and future therapies) to understand the limits of CNS regeneration in mammals.

Organisms in the phylum Echinodermata hold a unique evolutionary position, that places them at a basal branch in vertebrate evolution. Their nervous system has been described by several investigators [14][15]. In brief, their CNS is composed of five radial nerve cords (RNCs), arranged around a central axis, that come together in an anterior nerve ring. The radial nerves are ganglionated containing neuronal and glial cell bodies surrounding a central neuropil area [16]. However deceptively simple this arrangement may seem, various subpopulations of cells give these tissues amazing functional complexity, even in the absence of cephalization or specialized nervous structures. Furthermore, these organisms are capable of extensive CNS regeneration [17][18]. The regenerative capabilities, relatively simple anatomy, and close relation to vertebrates make these organisms ideal models for biomedical studies on CNS regeneration. Particularly, they allow researchers to study the mechanisms by which, following injury, the animals minimize neurodegeneration and trigger a regenerative process.

The brown rock sea cucumber, *Holothuria glaberrima*, has been a particular focus of studies in the past. These studies include morphological characterization of the regenerating RNC structures, as well as the description of the cellular events that underlie the regeneration process [17]. One of the main findings arising from these studies is the essential role that radial glia-like cells play in mediating CNS regeneration by giving rise to neurons and other cells through dedifferentiation and proliferation [18][19]. Although these studies thoroughly describe the cellular events that unfold during RNC regeneration and the distinct populations of cells present during various regenerative stages, there is limited information on the molecular events that occur during regeneration. Mashanov and colleagues provided an overview of the transcriptomic changes during RNC regeneration at various stages in *H. glaberrima* (particularly 2, 12, and 20 days post-injury), as well as the groups of genes that were found to be differentially expressed [1]. However, the study suffers from a possible confounding effect, as the tissues for transcriptomic analysis were not exclusively RNCs. Due to the anatomical structure of the RNCs in holothurians, surgical extraction of an isolated RNC is practically impossible and the RNC dissection includes mRNA from the surrounding connective tissues, body wall muscles, and water vascular canal, among others. This can lead to a misidentification of the differentially expressed genes found at each stage, as the genes may be differentially expressed in some other tissue, but not the actual RNC.

We have now developed a protocol to isolate *H. glaberima* RNCs by collagenase treatment [20]. This technique allows an almost complete isolation of RNCs from surrounding tissues, thus producing a source of CNS tissue with little or no contamination from adjacent tissues. The protocol, nonetheless, is somewhat abrasive, and produces an acute stress response on the isolated RNCs akin to the initial response to trauma experienced by the RNC after injury. Therefore, we have used this protocol to characterize the molecular basis of this stress response to understand the initial response to trauma of animals that exhibit extraordinary capabilities for CNS regeneration.

Results and Discussion

Stress response genes of the holothurian central nervous system

To identify genes of interest involved in the holothurian CNS stress response, we compared the gene expression of RNCs following their dissection and extraction from the body wall by a 24-hour collagenase treatment with that of RNCs explants kept in culture following 3 days after collagenase dissection [20]. The rationale behind this experiment was that the transection of the RNCs from anterior and posterior regions and from the peripheral nerves, together with the 24 hr collagenase treatment would induce a stress response on the RNC cells that would be ameliorated as the tissues are kept in tissue culture for the next 3 days. Differential gene expression analysis was performed using the

 doi:10.20944/preprints202210.0087.v1

DESeq2 R package [21]. We identified 422 genes with a significant increase in expression ($\log_2$ Fold Change $\geq$ 2 and FDR-adjusted p-value < 0.05) at 24 hours post-collagenase treatment, relative to the level of expression at 3 days in tissue culture. Conversely, we identified 454 genes that showed a significant decrease in expression ($\log_2$ Fold Change $\leq$ -2 and FDR-adjusted p-value < 0.05) during the same time frame (**Figure 1**).

Differentially expressed genes were then used to create two fasta files for annotation using a Python script provided by the developers of the *Corset* software [22]. The two fasta files were then annotated using the *BLAST* command line tool [23], the Uniprot peptides database used as our reference database [24]. The 30 genes with the most significant differential expression annotated using the Uniprot database are presented in **Table 1**.

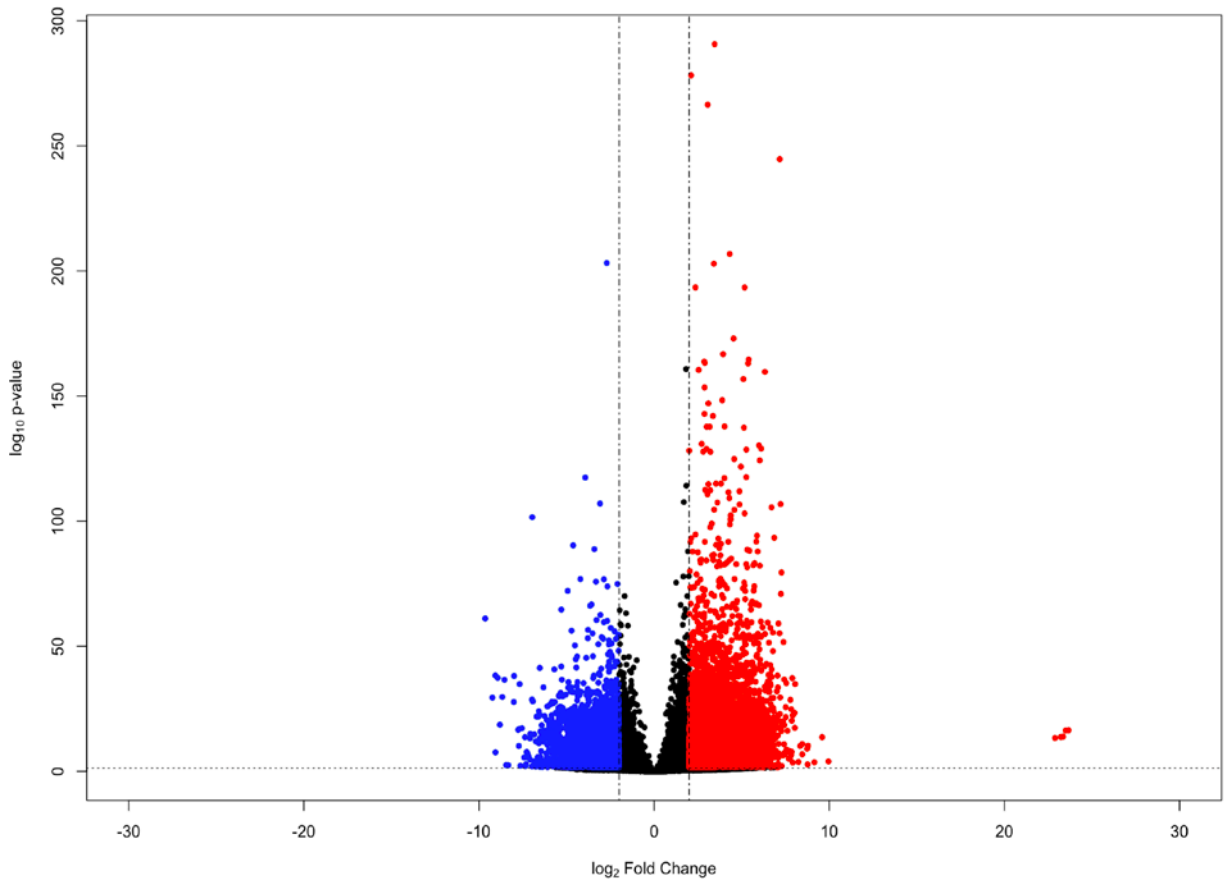

Figure 1: MA plot of genes in the holothurian CNS. Each point in the plot represents an individual gene. Points colored red represent upregulated genes ($\log_2$ Fold Change $\geq$ 2 and FDR-adjusted p-value < 0.05), while points colored blue represent downregulated genes ($\log_2$ Fold Change $\leq$ -2 and FDR-adjusted p-value < 0.05).

Functional groups of genes involved in the stress response of the holothurian Central Nervous System

Functional groups of genes were identified according to Gene Ontology (GO) Consortium terminology. For upregulated genes, enriched terms in Molecular Functions (MF) included Unfolded Protein Binding, Peptidase Activity, and Transmembrane Receptor Activity. Biological Process (BP) enriched terms ranged from Cellular Response to Stimulus, and Proteolysis, to Cell Adhesion. Finally, enriched terms in Cellular Components (CC) included Membrane Part, and Integral Component of Membrane (transmembrane protein) (**Figure 2a**).

Conversely, enriched terms in MF for downregulated genes included RNA Polymerase Activity, Oxidoreductase Activity, and Transferase Activity. BP enriched terms en-

 doi:10.20944/preprints202210.0087.v1

compassed RNA Processing, ncRNA Processing, and Ribosome Biogenesis. Lastly, CC enriched terms ranged from Mitochondrial Envelope to Intracellular Organelle Part, and Membrane Protein Complex (**Figure 2b**).

These initial analyses provided a broad overview of the most prevalent processes during the CNS stress response in *H. glaberrima*. The enriched GO terms served to identify genes that were associated with certain cellular processes of the stressed tissues by either increasing or decreasing their expression. It is interesting to compare these results with those obtained after holothurian RNC transection *in vivo* [1]. In fact, there is little if any similarity among the processes defined by their gene expression profile. *In vivo*, most processes 2 days after transection, correspond to processes associated with extracellular matrix or with muscle systems. The reason behind this is that, *in vivo*, the RNC is embedded within the body wall and it is practically impossible to isolate the tissue by itself. Thus, the *in vivo* results most probably represent the ongoing changes in the body wall tissues with little if any contribution from the RNC. In this respect, our present results, showing biological terms associated with the response to various stressors correspond to a factual view of what is taking place within the RNC neuronal and glial cells after transection, since little or no other tissue contamination is present in our *in vitro* explants.

The enriched terms, however, give only a general idea of what is occurring at a molecular level during the stress response. To provide a more accurate description of the factors involved, we surveyed the RNC transcriptome database for homologs that matched classical stress actors in ubiquitination, apoptosis, and unfolded protein responses, along with other recently described families of stress-associated proteins such as the stress-protective factors *Hero* [25].

Preprints (www.preprints.org) | NOT PEER-REVIEWED | Posted: 8 October 2022 doi:10.20944/preprints202210.0087.v1

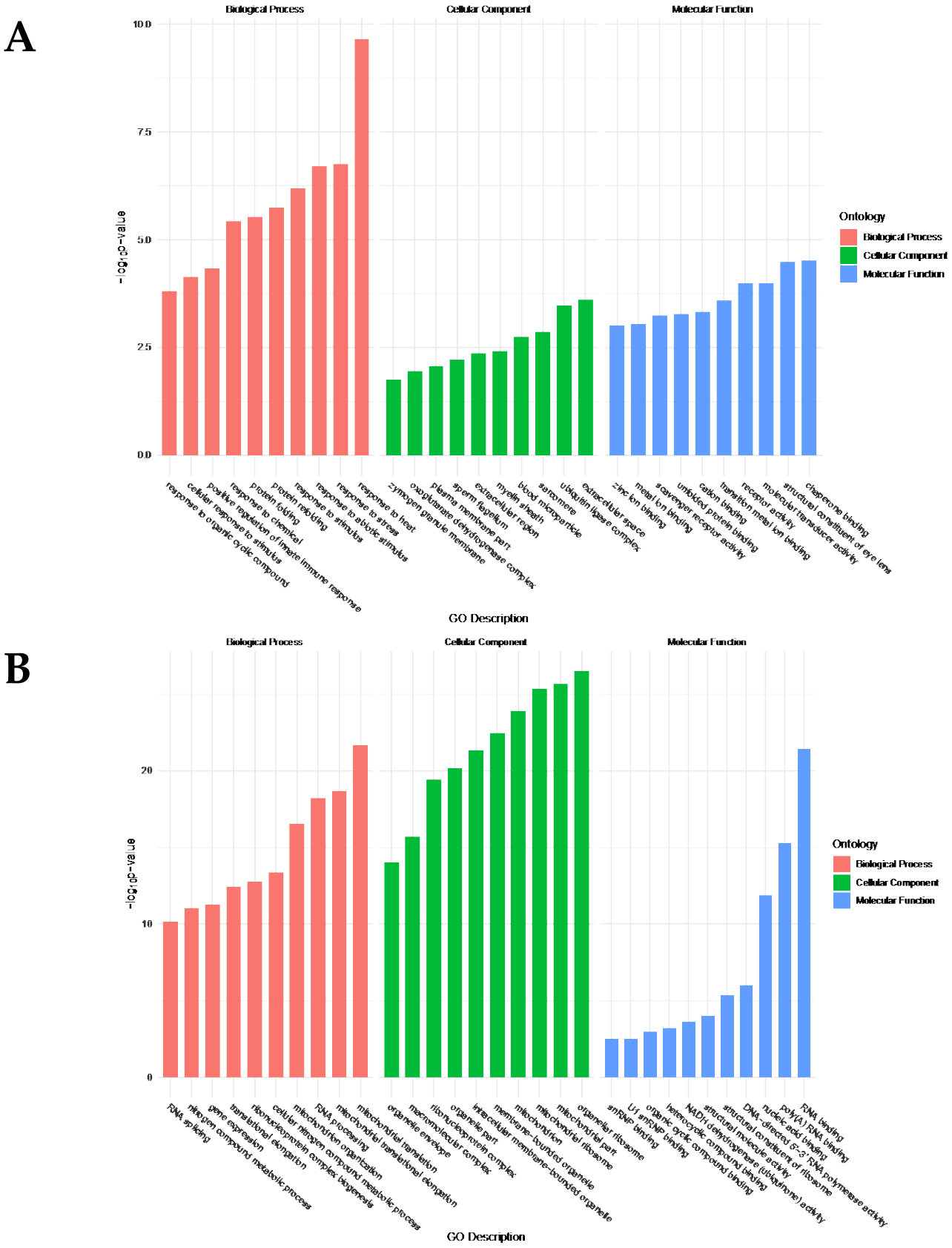

Figure 2: Bar plots showing top ten enriched functional terms for genes upregulated (**a**) and downregulated (**b**), at 24 hours post-collagenase treatment.

Preprints (www.preprints.org) | NOT PEER-REVIEWED | Posted: 8 October 2022 doi:10.20944/preprints202210.0087.v1

Table 1 Genes with most significant differential expression

Gene	Uniprot Accession ID	Function	Pattern of Expression (vs Day3)
RAB12	Q6IQ22	Signal Transduction	Downregulated
THOC6	Q86W42	Protein Binding	Downregulated
HSP40B	Q3HS40	Unfolded Protein Binding	Upregulated
TTLL7	A4Q9F0	Cellular Protein Modification Process	Upregulated
POLYQ	P23398	Protein Binding	Upregulated
RPS27A	P62979	Structural Constituent of Ribosome	Downregulated
HSPA1A	P0DMV8	Damaged DNA Binding	Upregulated
TBC1D15	Q8TC07	Rab GTPase Activator Activity	Upregulated
EGR1	A4II20	Differentiation and mitogenesis	Upregulated
BCDO1	Q9HAY6	Vitamin A Metabolism	Upregulated
NEURL1	Q0MW30	E3 Ubiquitin Ligase	Upregulated
HSPA2	P54652	Unfolded Protein Binding	Upregulated
JUN	P54864	Transcription Factor	Upregulated
CBLIF	P27352	Cobalamin Binding	Downregulated
RPS5	P46782	Structural Constituent of Ribosome	Downregulated
MRPL12	Q7YR75	Structural Constituent of Ribosome	Downregulated
SPDEF	O95238	Transcription Factor	Downregulated
DMBT1	Q9UGM3	DNA Binding	Upregulated
BAG3	O95817	Heat Shock Protein Binding	Upregulated
DYRK2	Q5ZIU3	Regulation of Cell Growth and Development	Upregulated
WARS2	Q9UGM6	Mitochondrial tRNA Ligase (Tryptophan)	Downregulated
SLC6A1	P30531	GABA Transporter	Upregulated
TIMM8A1	Q9WVA2	Mitochondrial Intermembrane Chaperone	Downregulated
AP5S1	Q9NUS5	Endosomal Transport	Downregulated
JRKL	Q9Y4A0	DNA Binding	Downregulated

Preprints (www.preprints.org) | NOT PEER-REVIEWED | Posted: 8 October 2022 doi:10.20944/preprints202210.0087.v1

NETO2	Q8NC67	Ionotropic Glutamate Receptor Binding	Upregulated
LZIC	Q8WZA0	Beta-Catenin Binding	Downregulated
NRL	P54846	Transcriptional Regulator	Upregulated
FAM171B	Q6P995	Integral Component of Membrane	Downregulated

Note: All genes have an adjusted *p*-value of < 0.05.

Heat Shock Proteins

The Heat shock protein (Hsp) family has been associated, not only with heat-induced stress, but also to stress originating from multiple other environmental factors. This protein family is divided into five groups according to their size and sequence similarities: the 60-, 70-, 90-, 100- kDa Hsps and the small size Hsps (sHsps). Therefore, we decided to look for sequences that matched these and other members of the Hsp family, as well as additional proteins commonly associated with Hsp family members. As expected, potential homolog sequences were highly represented in our transcriptome and showed significant upregulation after 24 hours of collagenase treatment.

We identified one putative *Hsp20* sequence in the RNC transcriptome database. The sequence was similar to the *Hsp20* sequence of the purple sea urchin *Strongylocentrotus purpuratus*. The sequence showed upregulated expression after collagenase treatment.

We next focused on *Hsp90* homologs. We found one sequence similar to the *Hsp90* protein (**Figure 3)** that aligned with a cytosolic *Hsp90* protein from *A. japonicus*. We were unable to detect isoforms of the *Hsp90* proteins that are found in the mitochondria or endoplasmic reticulum [26]. The aforementioned contig was found to be significantly upregulated 24 hours after RNC transection and collagenase treatment.

In our probe, we also found a contig with very high similarity to the chaperone *DNAJA1B* (also known as *Hsp40*) protein of *A. japonicus*. This contig was complete and possessed significant upregulation of expression after RNC transection and enzymatic dissection. A second partial sequence with significant homology to *DNAJ*, and distinct from the first contig, was also found to be upregulated after collagenase treatment.

Rounding off our search for members of the classical Hsps, we probed the transcriptome for *Hsp70* homologs. For this class of *Hsps*, we found 5 distinct contigs (28% homology, 19% identity amongst themselves), all similar to *Hsp70* proteins from various organisms. An alignment of the conserved *Hsp70* functional domain of the 5 sequences is shown in **Figure 4**. Two of these contigs contained a complete sequence, meaning they possessed an initial Methionine and a stop codon, while the remaining sequences were partial. All of the aforementioned contigs, whether complete or partial sequences, possessed significant upregulation of expression at 24 hours post-collagenase treatment. The identification of various distinct *Hsp70* family members in the RNC transcriptome of the *H. glaberrima* is consistent with the literature on this family of proteins, where multiple isoforms have been identified for *D. melanogaster*, *C. elegans*, *Ciona intestinalis*, and *H. sapiens* [27]. In fact, several Hsp have been characterized from different sea cucumber species. Among these are Hsp 90, Hsp 70, Hsp 60 and members of the small Hsp family [28][29][30][31][32]. These genes have been reported to be expressed by cells in the intestine, coelomocytes and many other tissues. Similarly, they are differentially expressed during stress, mainly due to temperature, salinity, hypoxia, or immune activation. Still, few reports associate these genes with regenerative processes, and none shows their expression in the nervous components of echinoderms. Some of the relevant findings are reports demonstrating Hsp72 upregulation in the regenerating arms of crinoids, another echinoderm class [33] and the changes observed in various Hsps during wound healing in the sea cucumber *H. tubulosa* [30].

 doi:10.20944/preprints202210.0087.v1

We also searched for less known chaperones or putative heat shock proteins. In this probe, we identified a homolog for the Sacsin chaperone in the RNC transcriptome. The contig is similar to the *DNAJC29* Sacsin from *H. sapiens* and *M. musculus*. This protein is a regulator of the *Hsp70* machinery and therefore an important regulator of stress. Particularly, the interplay between *Hsp70* and various co-chaperones has been shown to protect from neurotoxicity by promoting ubiquitination and degradation of misfolded proteins to prevent aggregation in models of neurodegenerative diseases [34][35].

While many chaperone proteins are upregulated following RNC dissection, we identified some exceptions to these findings. The first example to catch our attention was a homolog for *CALR*, which encodes the Calreticulin protein. This expression pattern is paradoxical, because Calreticulin is another important quality control mediator, specifically in the endoplasmic reticulum. This is made all the more striking when one considers that this protein is necessary for survival post-stress in *Caenorhabditis elegans in vivo* [36]. A possible explanation might be that Calreticulin is necessary for long-term stress response and that its levels remain elevated in the explant after 3 days of the dissection by the collagenase treatment.

Other downregulated factors that caught our attention were various mitochondrial chaperones. Among these were homologs for *BCS1* and *TIMM10*. Both contigs were significantly downregulated after transection and 24 hours post-collagenase dissection. These data, along with the data shown in **Figure 2B**, suggest a depletion of mitochondrial activity in these cells following stress. Davis *et al*. [37] and Hayakawa *et al*. [38] have described a phenomenon by which neurons transfer damaged mitochondria to surrounding glial cells for lysosome degradation. This form of cell-to-cell signaling could potentially explain the depletion of mitochondrial transcriptomic activity at 24 hours post-collagenase treatment. And because this transfer of mitochondria is two-sided, meaning that neurons may receive new mitochondria from glial cells, this could also explain the observed cell viability and low apoptotic index.

The protective effect of individual Hsps might vary depending on the stress factor and on cell type. Nevertheless, there are several reports where the expression of Hsps is associated with nervous system development and/or with its protection during disease, injury or other stressors [39][40][41][42]. Some of the Hsps proposed nervous system roles, including: suppressing inflammation, increasing survival, modulating differentiation and/or neurogenesis, could be crucial for the holothurian CNS neurons during regenerative processes.

In summary, we detected that, with the exception of Calreticulin and mitochondrial-specific chaperone proteins, Hsps are mostly upregulated following CNS transection and enzymatic dissection, a fact that suggests an essential role for these types of protein factors in the stress response of the holothurian CNS.

Preprints (www.preprints.org) | NOT PEER-REVIEWED | Posted: 8 October 2022 doi:10.20944/preprints202210.0087.v1

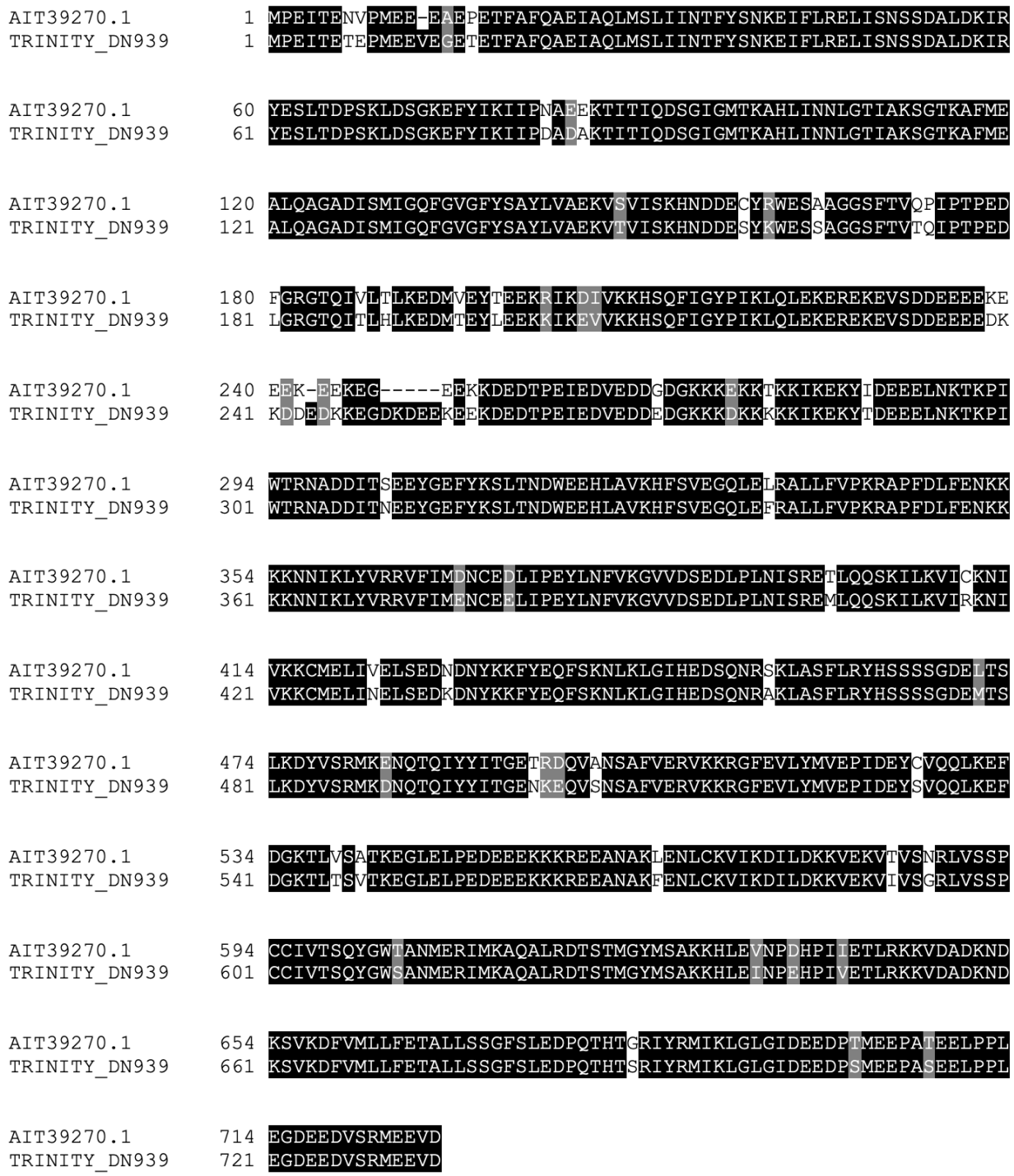

Figure 3: Alignment of *Hsp90* homolog identified in the RNC transcriptome with a *Hsp90* sequence from *A. japonicus*.

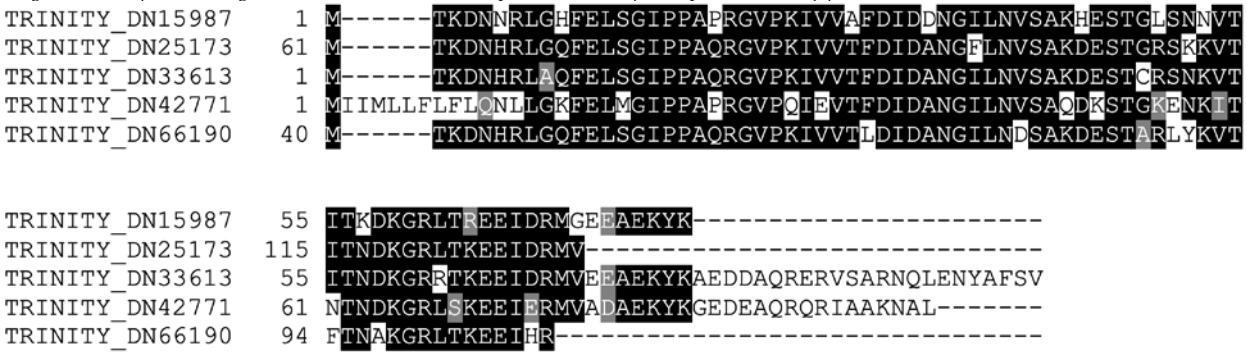

 doi:10.20944/preprints202210.0087.v1

Figure 4: Alignment of the conserved domains of the *Hsp70* homologs identified in the RNC transcriptome.

Ubiquitin

Chaperones are known to promote the ubiquitination and degradations of misfolded proteins. Thus, it is not surprising that we found that many of the proteins associated with the ubiquitin proteasome system are also upregulated following RNC enzymatic dissection. The ubiquitin pathway is inextricably associated with stress responses at the molecular level in higher eukaryotes. The pathway plays an important role in damaged protein disposal during stress responses to prevent harmful protein aggregation and to help restore homeostasis in the long-term [43]. Previous work from our group and others have provided insights on the role that this pathway may play in stress responses of echinoderms [44][45][46]. Using these previous studies to confirm what we observed in our NGS data, we decided to survey various components of this pathway, and other ubiquitin-associated factors, in our RNC transcriptome. We found various matches for ubiquitin and polyubiquitin to be upregulated 24 hours post-collagenase treatment, as well as various protein factors involved in the ligation of ubiquitin to defective protein products. Among these were RBBP6, RNF31, UBE3C-E3, TRIM2, and β-TrCP. We also identified the upregulation at 24 hours post-collagenase treatment of various protein factors known to be associated with the ubiquitin proteolysis pathway. These factors include DYRK2 and ZFAND2B. Conversely, we identified inhibitors of ubiquitination among the downregulated genes at 24 hours post-collagenase treatment. Such genes include NOP53, UBLCP1, and BABAM1. From this list of downregulated genes, we also identified various factors involved in protein ubiquitination, such as UBFD1, UBE2C, STUB1, CUL5, and UBE2U. Finally, we identified a transcript with similarities to STUB1 with a significant downregulation of expression. This particular transcript encodes an E3 Ubiquitin-ligase, which was the only transcript of an E3 ligase to be downregulated at 24 hours post-collagenase treatment.

In these analyses, we identified 13 transcripts with similarity to Ubiquitin that were upregulated 24 hours post-collagenase treatment. To elucidate the uniqueness of each of these transcripts, we aligned all 13 translated transcripts using the Geneious software. This alignment showed the transcripts formed three subgroups. The first subdivision contained a single sequence including an initial Methionine and stop codon. The second subdivision contained two sequences that shared 50% similarity between each other, but less than 50% similarity with the rest of the surveyed transcripts; only one of these sequences contained an initial Methionine, but no stop codon. And finally, the third subdivision had 9 sequences that were 43% similar and 39% identical amongst themselves. From these 9 sequences, we selected the most representative sequence based on its length and the sequence similarity it shared with the sequences from the other two sequence subdivisions. The remaining 8 sequences might represent distinct alleles or sequencing errors, and we therefore decided to focus only on one sequence from this group for the present study. In summary, we identified at least four distinct transcripts that encode different Ubiquitin proteins in *H. glaberrima* (**Figure 5**). The possibility that other ubiquitin isoforms are present is very likely, since our analysis was highly conservative trying to identify only the most distinct unique sequences.

As ubiquitination for proteasomal degradation is a common molecular hallmark of stress in eukaryotes, we expected many components of this pathway to be significantly upregulated at 24 hours post-collagenase treatment. Consistent with our expectations, many upregulated factors included the genes that code for the actual ubiquitin and polyubiquitin molecules, as well as various proteins involved in ubiquitin ligation. Our data also uncovered a complex network of these proteins, where some ubiquitin ligases are upregulated, but others experience significant downregulation during the CNS stress response. We hypothesize that this molecular process within the cells of the holothurian CNS involves the ubiquitination of only specific groups of proteins.

Preprints (www.preprints.org) | NOT PEER-REVIEWED | Posted: 8 October 2022 doi:10.20944/preprints202210.0087.v1

The identification of at least four distinct Ubiquitin transcripts further supports the idea of intricate regulation of proteasomal degradation, as the four transcripts share a certain degree of similarity (owed to their Ubiquitin domain), but with an interesting grade of difference in the remaining sequence. Such differences in sequence composition are a classic biological mechanism for specificity, particularly by binding specificity and affinity. Another interesting possibility is that some of these transcripts might be pseudogenes. One such pseudogene (*UBBP4*), with Ubiquitin domains, that is actively transcribed was recently described by Dubois *et al*. [47] While we identified at least four transcripts, we do not rule out the possibility of more transcripts being present in our RNC transcriptome, be they protein-coding variants that allow further specificity, or pseudogene transcripts with yet to be described functions.

Following up on the identification of various upregulated Ubiquitin transcripts at 24 hours post-collagenase treatment, we logically expected to find that E3 ubiquitin-ligases, the final effectors of the ubiquitin-tagging modification, would follow the same pattern of transcript abundance. This was true, to a certain extent, given our identification of three such E3 ligases that were upregulated at 24 hours post-collagenase treatment:_RNF31, UBE3C-E3, and TRIM2.

An exception to the expression patterns observed for most of the E3 ubiquitin-ligases was that of STUB1. While all the other E3 ligases were upregulated at 24 hours post-collagenase treatment, STUB1 was downregulated at this timepoint. A possible explanation for this finding is that STUB1 is a versatile protein with various roles to play in the stress response. Among these functions is E4 ligase-like activity, wherein this protein regulates other E3 ligases in the stepwise process of ubiquitination and proteasome degradation [48]. Therefore, the time of action for STUB1 in the RNC stress response may be later than that of the other E3 ligases because of functional plasticity. It is also worth pointing out that STUB1 has also been found to mediate ubiquitination of Hsp70 and Hsp90 chaperones for proteasomal degradation [49]. The pattern of expression found for STUB1 then is consistent with the upregulation of these chaperones in the RNC transcriptome at 24 hours post-collagenase treatment.

Figure 5: Alignment of the translated ORFs of the four distinct transcripts from the *H. glaberrima* RNC transcriptome that matched Ubiquitin.

Apoptosis

Programmed cell death or apoptosis is closely related to cellular stress responses. It was, therefore, important to determine the expression of genes associated with apoptosis in our transcriptomic data. Several apoptotic related genes, namely *TRAF3*, *AP-1*, *SQSTM-1*, *BAK1*, *CCAR1*, and *LAMTOR-5*, were found to be differentially expressed (**Table 3**).

 doi:10.20944/preprints202210.0087.v1

However, several other apoptosis-related genes, namely *BIRC5* (*survivin*), a member of the *IAP* family, *BCL-2*, and *p53*, although found in our transcriptome, showed no significant differential expression. Similarly, a search for caspases (as these proteins are some of the main effectors of cell death) in our transcriptome identified homologs for caspases 1-3 and 6-8 but none were differentially expressed. These data appeared paradoxical at first glance, with some apoptotic genes showing differential expression while others showing no change in expression. In brief, it provided no clear clue of whether apoptosis was being induced by the stress response or not. To settle the issue, we performed a TUNEL analysis to quantitate apoptosis at the cellular level. In both collagenase treated tissues (24 hrs) and explants left for 3 days in culture we found a small number of apoptotic cells in RNC explants, the apoptotic index being quite low (< 1%) (**Figure 6**), a finding that may be explained in great part due to the action of chaperones [50]. Thus, taken together, our data suggest that while some genes in the apoptosis pathway are differentially expressed, apoptosis is not actively occurring during the stress response. This observation was surprising, as stress is commonly known to mediate cell death through careful orchestration by the endoplasmic reticulum and the unfolded protein response (UPR). Studies from mammals indicate that modulation of apoptosis exerted by the UPR may be responsible for this paradoxical outcome [51]. In fact, we have found XBP1, a factor involved in the UPR, that was upregulated at 24 hours post-collagenase treatment. A contig homologous to *XBP1* was found to be significantly upregulated at 24 hours post-collagenase treatment. *XBP-1* encodes a transcription factor essential for the UPR in the ER. Specifically, the activated *XBP-1* protein regulates a range of transcriptional targets, including *GATA3*, *MYC*, and *FOS* [52]. In this process, the *XBP1* transcription factor can act as a "switch" between apoptosis and survivability by regulating its downstream effectors. In various Alzheimer's Disease models the active form of *XBP-1* shows neuroprotective activity by way of preventing amyloid-beta neurotoxicity after ER stress [53], a fact that highlights the importance of this factor in the prevention of stress-mediated neurodegeneration. This is, to our knowledge, the first evidence of elements of this apoptosis repression pathway and its associated physiological response being present in echinoderms. The broader implications of these data will be of great interest for future work, given that we have shown that RNCs that are transected and treated with collagenase for 24 hours display many of the traditional hallmarks of stress (widespread ubiquitination, Hsp activation), but avoid the pitfall of apoptosis. Future experiments in our laboratory will provide data for appropriate comparisons of this apoptosis repression response in *H. glaberrima* to that of other mammals in which it has been described comprehensively.

A

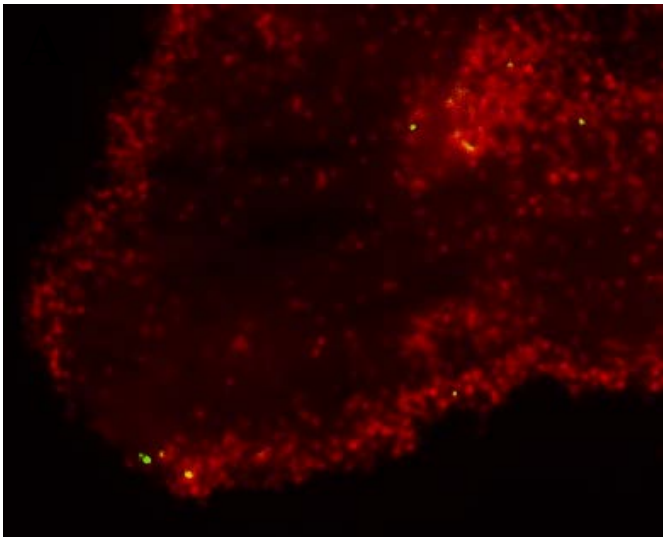

Preprints (www.preprints.org) | NOT PEER-REVIEWED | Posted: 8 October 2022 doi:10.20944/preprints202210.0087.v1

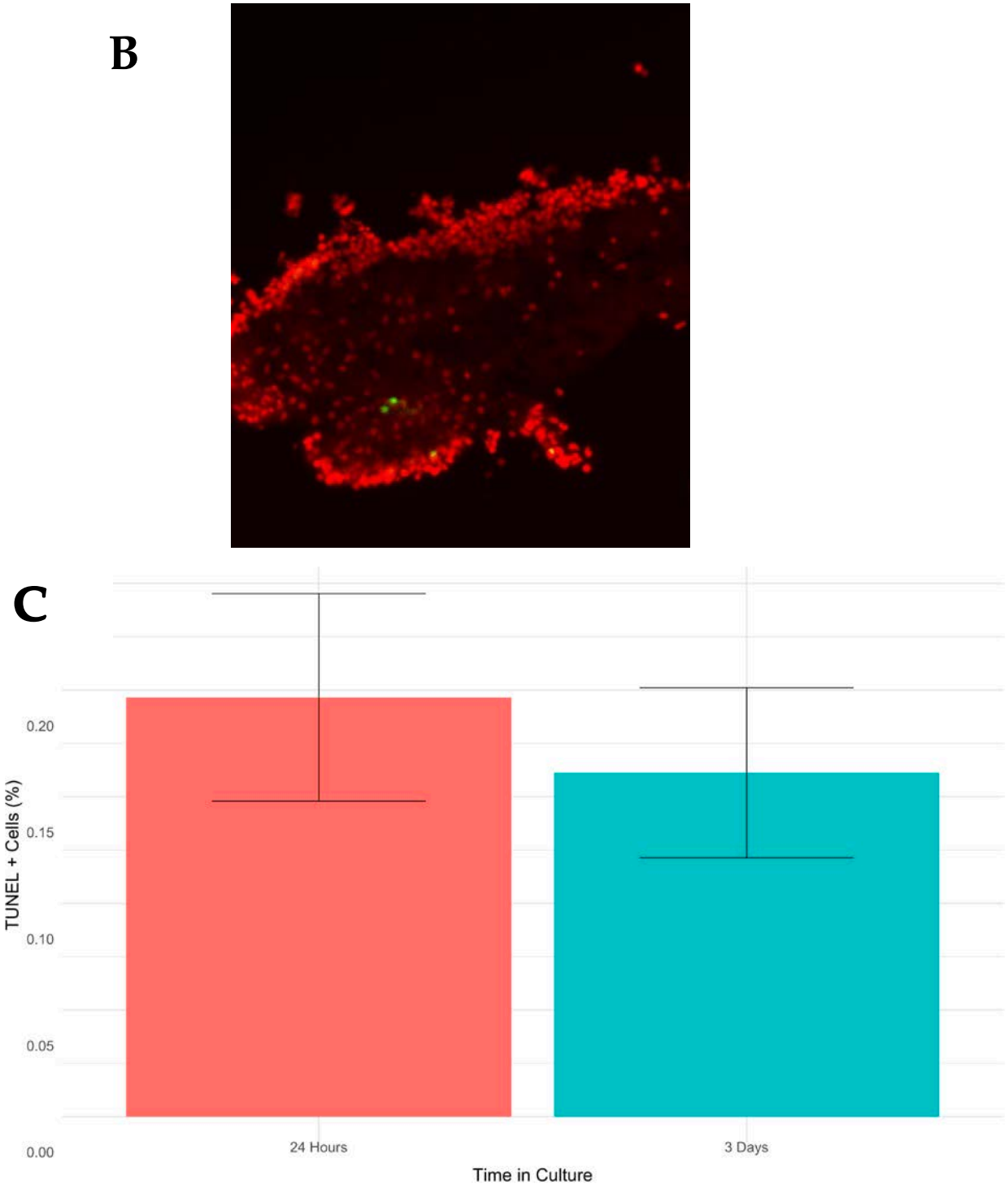

Figure 6: Micrographs of RNC explants at 3 days post-collagenase treatment (**A**) and 24 hours post-collagenase treatment (**B**). Cell nuclei were stained with DAPI (red), and apoptotic cells were detected using TUNEL (green). Finally, the percentage of apoptotic cells in RNC explants placed in culture for 24 hours and 3 days was calculated (**C**).

Preprints (www.preprints.org) | NOT PEER-REVIEWED | Posted: 8 October 2022 doi:10.20944/preprints202210.0087.v1

Table 3 Apoptosis-related Genes in the RNC Transcriptome

Gene	Gene Function	Pattern of Expression (vs Day3)
TRAF2	Apoptosis Inhibitor	Upregulated
AP-1	Transcription factor involved in controlling proliferation, apoptosis, and proliferation	Upregulated
SQSTM-1	Promotes Autophagy	Upregulated
BAK1	Promotes Apoptosis	Upregulated
CCAR-1	Regulates cell division cycle and apoptosis	Upregulated
HK1	Carbohydrate metabolism and maintenance of outer mitochondrial membrane	Downregulated
LAMTOR-5	Inhibits Apoptosis	Downregulated
BIRC5	Apoptosis Inhibitor	No significant change
XIAP	Apoptosis Inhibitor	No significant change
BCL-2	Apoptosis Regulator	No significant change
p53	Apoptosis Inhibitor	No significant change
CASP1-3 and *6-8*	Apoptosis Mediators	No significant change

Note: Differential expression significance threshold was set at adjusted *p*-value of < 0.05.

Other stress related genes

Retrotransposons

Retrotransposons have been implicated in the response of cells to stress [54]. In previous experiments, Mashanov and colleagues identified a series of long terminal repeat (LTR) retrotransposons in the radial nerve cords of *H. glaberrima* [55]. Since the involvement of these LTR retrotransposons in neural regeneration was a key finding of their work, we decided to survey the presence of the 36 sequences in our transcriptome database. We found all 36 LTR sequences. However, only two of the sequences were differentially expressed relative to the *Day3* group: *Gypsy-19* and *Gypsy-1*, with the former being upregulated and the latter downregulated. *In vivo*, it was shown that the expression of most retrotransposons remains high for 1-3 weeks, thus it is possible that in our *in vitro* explants, the expression remains high and therefore shows no difference from the recently injured/enzymatically dissociated RNC. In this respect it is interesting that *Gypsy-19*, *in vivo*, is one of the few transposons that shows and acute response increasing almost 4-fold 2 days after injury, but then going back to uninjured levels by the following week.

Hero proteins

 doi:10.20944/preprints202210.0087.v1

Recently, Tsuboyama *et al*. [25] described the *Hero* protein family, a group of heat-soluble molecules found in non-extremophilic organisms. These proteins function as shields for heat-susceptible proteins, protecting them under stressful conditions such as heat-shock and desiccation, and thus counteracting protein denaturation. Moreover, this family of proteins plays a role in preventing neurodegeneration; in *Drosophila melanogaster* neurodegeneration models, these proteins block the pathological aggregation of proteins observed in various neurodegenerative diseases. Because this family of proteins shows promise for studies of neural diseases, we decided to search for homologs in the transcriptome of the isolated RNCs.

To perform this search, we used the BLAST software, querying the RNC transcriptome with the Uniprot database (which itself holds the *Hero* protein sequences). As the *Hero* protein family is not necessarily defined by a specific primary structure or motif, it is difficult to identify homologs in *H. glaberrima* for this novel family of proteins. Nevertheless, we have identified three homologs in the radial nerve cord transcriptome. Two of the homologs (*Hero45*, *Hero11*) did not experience significant differential expression at 24 hours post-collagenase treatment, and the homolog that did experience significant differential expression (*Hero7*) was downregulated post-collagenase treatment. This observation contrasts with our expectations for the role these proteins play in neurodegeneration.

Integrated Stress Response

The integrated stress response (ISR) pathway has been described as an important mechanism used by eukaryotic cells to mitigate cell extrinsic (e.g., nutrient deprivation) and intrinsic (e.g., ER stress) stressors [56]. Pathway initiation is regulated by phosphorylation of eukaryotic translation initiation factor 2 alpha (eIF2α) via PERK, PKR, HRI, GCN2 kinases [57]. Once eIF2α is phosphorylated global protein synthesis is reduced and survival and recovery genes, such as activating transcription factor 4 (ATF4), are selectively translated [56]. Given the physiological stress exerted to *H. glaberrima* RNC, we evaluated ISR pathway involvement by assessing 10 main ISR factors (**Table 6**). All except C/EBP homologous protein (CHOP) were found in our transcriptome database. To our surprise none of the listed factors showed differential gene expression compared to RNC explant cultured 3 days post-collagenase treatment. These results are consistent with our previous data. It is well known that apoptotic factors p53, BCL-2, and caspase-1 are effectors of the ISR pathway none of which showed significant differential expression. Therefore, the accumulation of these results suggests no active ISR signaling pathway in collagenase treated RNC.

Preprints (www.preprints.org) | NOT PEER-REVIEWED | Posted: 8 October 2022 doi:10.20944/preprints202210.0087.v1

Table 6

Factors	Factor Name	Response	Pattern of Expresion
ATF4	Activating Transcription Factor 4	Cell survival and recovery during ISR. ISR effector and master transcription factor.	No significant change
PERK	PKR-Like ER Kinase	Kinases that initiate the ISR reponse by phosphorylating eIF2α translation initiation factor.	No significant change
PKR	double-stranded RNA-dependent Kinase		No significant change
HRI	Heme-regulated eIF2α Kinase		No significant change
GCN2	General control non-derepressible		No significant change
IRE1	inositol-requiring protein 1	Initiates the UPR (Unfolded Protein Response)	No significant change
ATF6	activating transcription factor 6	Initiates the UPR (Unfolded Protein Response)	No significant change
PP1	Protein Phosphatase 1	ISR termination signal	No significant change
eIF2a	eukaryotic translation initiation factor 2A	Phosphorylation of this factor commenzes ISR	No significant change
CHOP	C/EBP homologous Protein	CHOP/ATF4 interaction negatively regulates ATF4	Not Found

Transcription Factors

We identified various differentially expressed contig sequences homologous to an array of transcription factors (**Table 2**). Among these were *ATF2*, a transcription factor that dimerizes with *Jun* [58] to regulate cellular stress responses, including the DNA damage response [59]. *RXRA* was another upregulated factor identified in our transcriptome database. This factor is primarily a retinoid X receptor [60], but also shuffles between the nucleus, cytoplasm, and mitochondria. *RXRA* has been shown to translocate to dimerize with *NUR77*, after which it is translocated to the mitochondria, and *NUR77* interacts with *BCL-2* to induce apoptosis [61]. None of these transcription factors were reported to be differentially expressed after transection *in vivo* [1], probably due to what was explained earlier that in the *in vivo* studies other components (muscle, ECM) within the sample presented the larger gene expression changes.

Table 4 Transcription factors with significant differential expression

Gene	Pattern of Expression (vs Day3)
ATF2	Upregulated
RXRA	Upregulated
EF1A1	Upregulated
ZNFX-1	Upregulated
NR4A2	Upregulated

Note: All genes have an adjusted p-value of < 0.05.

Preprints (www.preprints.org) | NOT PEER-REVIEWED | Posted: 8 October 2022 doi:10.20944/preprints202210.0087.v1

Conclusions

It is important to place our results within the context of the experimental procedure and the tissue comparisons. For one, the stress elicited in our model system comes from two different procedures. On the one hand it involves the transection of the RNC from anterior and posterior regions of the radial nerve as well as the transection of peripheral nerves. On the other hand the tissue is kept in a collagenase solution for ~24 hrs and then dissociated from the surrounding body wall. Therefore, the protocol provides a very particular stimuli which may impact the expression of certain genes or signaling systems. The procedure can be compared to dissecting out portions of the spinal cord from the surrounding vertebra and cutting of the spinal nerves, then keeping them as explants in culture. Thus, some of the observed effects might be due to different "types" of stress, depending on the cells that might have suffered injuries or alterations in their neuronal circuits. Second, and most important, is that the tissue used for gene expression comparisons is the RNC kept in culture for three days following removal from the body wall by transection and enzymatic dissection. Comparisons to the *in situ* RNC are not possible, in view of the fact that the latter is embedded within the body wall of the animal, and it is impossible to surgically isolate it without contamination from the surrounding tissues, as has been shown in some of our comparisons. Therefore, it is plausible that some of the observed responses are due to additional changes induced by the culture environment. Nonetheless, experimental data from the laboratory have shown that RNCs kept in culture for up to 7 days maintain many of their morphological integrity and cell processes [20]. In addition, it is important to state that our comparative analyses implies that a gene that shows "no significant change" in its expression is either not changing at all in response to the dissection or on the contrary that its expression changes take place after the enzymatic dissection and continue even after 3 days in culture.

Having stated these provisions, it still is important to highlight that the profile of gene expression strongly suggests a stress response comparative to those detected in many tissues and animal species, but at the same time with a gene expression profile that might be distinctive to the holothurian RNC. Most importantly, we provide evidence of stress associated genes that are found within the holothurian nervous system transcriptome and show how some of these might be playing a role in the stress response (as determined by their changes in expression). Our work provides an important listing of those genes that should be further studied in order to determine how the stress associated with injury might elicit some of the mechanisms found in the holothurians that protect their nervous system and allows for its full regeneration.

Table 5 All genes mentioned in the body of this text and their respective change in expression

Gene	**Log_2 Fold Change**	FDR-adjusted p-value
RAB12	-3.52	0.0006
THOC6	-3.91	9.90E-06
HSP40B	6.67	1.75E-06
TTLL7	5.96	0.0002
POLYQ	3.24	0.0001

Preprints (www.preprints.org) | NOT PEER-REVIEWED | Posted: 8 October 2022 doi:10.20944/preprints202210.0087.v1

RPS27A	-4.71	0.0009
HSPA1A	5.48	3.32E-08
TBC1D15	5.40	1.25E-05
EGR1	6.75	3.62E-25
BCDO1	5.93	1.13E-16
NEURL1	4.79	3.77E-14
HSPA2	5.97	5.93E-13
JUN	4.55	1.31E-05
CBLIF	-4.76	1.66E-11
RPS5	-8.43	6.42E-09
MRPL12	-5.81	1.98E-08
SPDEF	-5.38	1.09E-07
DMBT1	5.93	0.0008
BAG3	4.77	6.05E-07
DYRK2	3.43	6.25E-07
WARS2	-4.43	0.0001
SLC6A1	4.33	7.71E-07
TIMM8A1	-5.78	9.03E-07
AP5S1	-4.67	1.22E-06
JRKL	-7.14	2.68E-06
NETO2	4.27	2.77E-06
LZIC	-4.23	3.12E-06
NRL	5.86	4.29E-06
FAM171B	-3.73	5.77E-06
HSP20	3.30	0.0002
HSP90	4.77	1.20E-07

Preprints (www.preprints.org) | NOT PEER-REVIEWED | Posted: 8 October 2022 doi:10.20944/preprints202210.0087.v1

HSP70_1	4.39	1.24E-05
HSP70_2	6.73	2.30E-08
HSP70_3	5.17	1.07E-07
HSP70_4	3.52	0.0002
HSP70_5	5.54	9.24E-07
DNAJC29	3.34	0.00023117
CALR	-5.59	5.90E-06
BCS1	-3.51	0.00016118
TIMM10	-4.97	3.85E-05
RBBP6	2.49	0.0007
RNF31	2.54	0.0004
UBE3C-E3	3.07	0.0008
TRIM2	3.58	0.0008
β-TrCP	4.43	0.0003
DYRK2	3.43	6.25E-07
ZFAND2B	4.11	3.48E-05
NOP53	-3.98	0.0008
UBLCP1	-2.53	0.0006
BABAM1	-3.99	0.0003
UBFD1	-4.00	0.0005
UBE2C	-4.45	0.0009
STUB1	-3.11	0.0009
CUL5	-3.28	0.0005
UBE2U	-4.39	4.29E-05
UBB_1	3.33	1.09E-05
UBB_2	3.15	1.25E-05

 doi:10.20944/preprints202210.0087.v1

UBB_3	3.20	0.00029068
UBB_4	3.87	1.20E-05
TRAF3	2.38	0.0006
AP-1	4.41	6.46E-07
SQSTM-1	2.47	0.0002
BAK1	2.88	0.0002
CCAR1	5.64	0.0008
HK1	-3.31	0.0004
LAMTOR-5	-4.58	0.0001
XBP-1	2.73	0.03
GYPSY-19	3.66	0.0001
GYPSY-1	-3.89	0.0002
HERO7	-2.62	0.001
ATF2	3.25	0.0006
RXRA	4.81	0.0009
EF1A1	4.41	6.91E-05
ZNFX-1	6.53	3.97E-06
NR4A2	2.91	0.0001

Materials and Methods

Sample Collection

Adult individuals of the sea cucumber *Holothuria glaberrima* were collected from the north coast of Puerto Rico. Specimens were then stored in sea water aquaria at room temperature for 24 hours. Samples from *H. glaberrima* specimens were collected by excising radial nerve cords (RNCs) along with surrounding tissues. The RNCs are anatomically located in close proximity to various tissue (such as connective structures, segments of the body wall, and segments of water-vascular canal), making a perfect isolation via surgery practically impossible. Given this limitation, we used a recently described protocol to isolate the RNC [20]. In brief, the excised tissue complexes were placed in collagenase for 24 hours. This treatment isolates RNCs by degrading the collagen composition of the surrounding tissue. The surgical transection of the RNC from other CNS structures and from

 doi:10.20944/preprints202210.0087.v1

the peripheral nerves incites a stress response from the nervous tissue, allowing characterization of the central nervous system (CNS) stress response in our model organism. Therefore, comparisons were made between RNCs that had been collagenase-treated for 24 hrs and RNCs that were cultured as explants for 3 days following the collagenase treatment.

RNA Extraction

Total RNA extraction was performed using phenol and chloroform standard reagents, as well as the RNeasy mini kit (Qiagen, Germany). The concentration and purity of the RNA was determined using the NanoDrop-1000 Spectrophotometer (Nano Drop Technologies, Rockland, DE). Various RNC fragments from 1-2 specimens were pooled together to gather RNA and were treated as individual samples. Thus, 5 biological replicates were prepared: three corresponding to the RNCs treated with collagenase for 24 hours (*0 day* group) and two corresponding to the RNCs cultured for 3 days (*3 day* group) following collagenase treatment.

RNA Sequencing

Prepared RNA samples were sent to the Sequencing and Genomics Facility of the University of Puerto Rico in Rio Piedras for library preparation and RNA sequencing as published before [62]. Libraries were prepared using the TruSeq RNA Library Prep Kit (Illumina, San Diego, CA). Subsequently, paired-end RNA sequencing was performed (Illumina NextSeq 500, Illumina). Raw sequencing reads from the Illumina platform were deposited at NCBI Sequence Read Archive (SRA) under accession number NCBI:SRAXXXXX (*number to be placed at a later date*).

De novo Assembly Pipeline

The *elvers* software was used for the majority of the RNAseq analyses performed on the RNC data. The standard workflow (*Eel Pond Protocol*) defined by the developers was followed. This includes quality filtering, quality assessment, k-mer trimming and digital normalization, *de novo* assembly, read quantification, and differential expression analyses. All transcriptome processing was performed with the *elvers* modules, except for transcriptome annotation and hierarchical clustering of assembled contigs, which were performed separately. Additional differential expression analyses were also performed without the use of the *elvers* differential expression analysis module.

Reads were quality trimmed using the *Trimmomatic* software. Illumina adapters, leading and trailing bases with quality < 2 were removed from the sequencing data, as well as reads shorter than 25 base pairs.

K-mer trimming and digital normalization for the quality-trimmed reads were performed to reduce the computational burden of transcriptome assembly. A Python script provided by the *khmer* module from the *elvers* software was utilized, with a k = 20. If a particular k-mer was identified more than three times in the data, it was removed, thus decreasing the amount of reads for assembly without forsaking the quality of the assembled transcriptome.

The *Trinity* software was utilized for transcriptome assembly. Quality and k-mer trimmed paired-end reads were provided as input, and default parameters were used to generate contiguous sequences.

Quality-trimmed reads from the five sequenced libraries were aligned to the assembled contigs using the *Salmon* software to quantify expression. The *–dumpEq* parameter was specified to obtain equivalence classes. These classes are necessary for contig hierarchical clustering via the use of the *Corset* software. This step aimed to solve the redundancy issue that is common to *de novo* transcriptome assemblers such as *Trinity*. The *Corset*

 doi:10.20944/preprints202210.0087.v1

software hierarchically clusters contigs based on shared reads and expression, summarizing read counts into clusters which could then be interpreted as "genes". *Corset* was utilized with default parameters.

To perform the differential expression gene analysis, the *DESeq2* R package was utilized. The comparison was made taking the *0 day* group as an experimental group and the *3 day* group as a control group. To define a gene as differentially expressed, we established a False Discovery Rate (FDR) threshold of < 0.05.

Transcriptome Annotation

The assembled RNC transcriptome was annotated using the BLAST command line software. The Uniprot database was utilized as reference for identification of sequences of interest. Homology for our contig sequences was defined via the use of two parameters: E-value < 1e-5 and 50% identity between the matched sequence in the Uniprot database and our contig sequence. Additional annotation for ubiquitin and Hsp family proteins was also performed using the NCBI non-redundant (nr) database, with the established parameters for defining matches.

Gene Set Enrichment Analysis and KEGG Pathway Enrichment

The *DAVID* (Database for Annotation, Visualization, and Integrated Discovery) software was used to perform functional annotation and thus identify groups of genes and molecular pathways that were significantly enriched during RNC stress response [63]. Particularly, the *RDAVIDWebService* R package was used to access the data available from *DAVID* databases within the R interface. The obtained IDs from the Uniprot BLAST were used as the gene background for enrichment analyses, and the following annotation categories were specified: "GOTERM_BP_ALL", "GOTERM_MF_ALL", "GOTERM_CC_ALL". The obtained GO terms were filtered using the Revigo software to eliminate redundancy of the functional enrichment terms [64].

TUNEL

For apoptosis measurements, RNCs were fixed in 4%paraformaldehyde and sectioned as reported previously [20]. Deoxynucleotidyl transferase-mediated dUTP nick end labeling (TUNEL) was performed to identify cells in the RNC explants that were undergoing apoptosis. FragEL DNA Fragmentation Detection Kit, Fluorescent - TdT Enzyme (Calbiochem, QIA39) was used and cells were quantified following the protocol previously adapted in our lab[20][65].

Acknowledgements

This study was supported by NIH-R21AG057974. SCG and EQD were funded by 5T34GM007821-40S1, 5R25GM061151-17, RGR was funded by ENDURE NIH-2R25NS08068, YMN was funded by NSF Bridge to the Doctorate Program Grant Number: HRD-1906130. The authors acknowledge the help from the Sequencing and Genomics Facility and the High Performance Computing Facility of the University of Puerto Rico that are supported by an Institutional Development Award (IDeA) from the National Institute of General Medical Sciences of the NIH under Grant Number P20GM103475. We also acknowledge help from the University of Puerto Rico.

Preprints (www.preprints.org) | NOT PEER-REVIEWED | Posted: 8 October 2022 doi:10.20944/preprints202210.0087.v1

Supplementary:

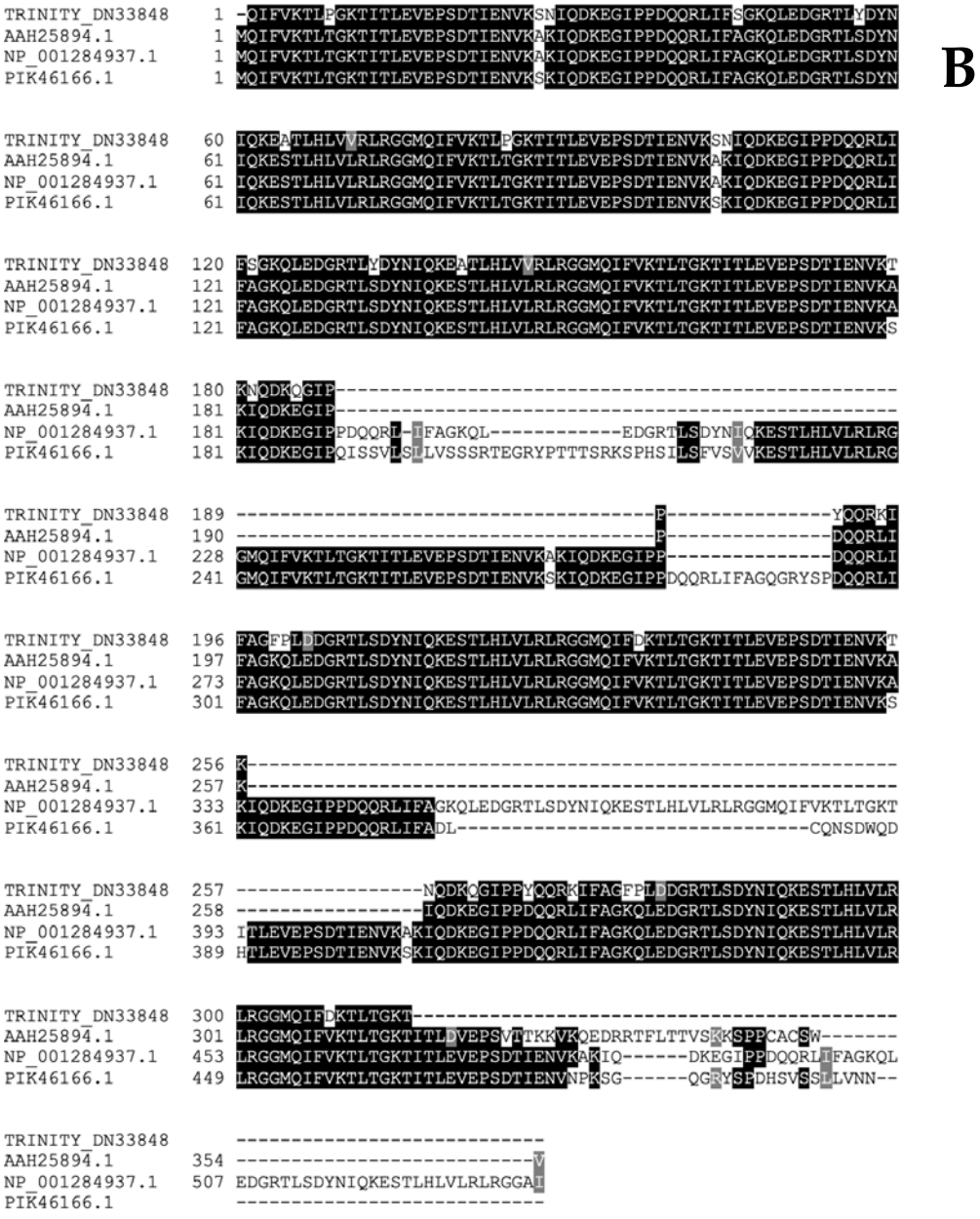

B

Preprints (www.preprints.org) | NOT PEER-REVIEWED | Posted: 8 October 2022 doi:10.20944/preprints202210.0087.v1

C

```
TRINITY_DN43805     1 ADGRSLYDFNLPKESTLHVVLRLRGCMQIFVNTLTGKTITLEVETSDTIENVKSKIQDKE
AAA28997.1          1 MQIFVKTLTGKTITLEVEPSDTIENVKAKIQDKEGIPPDQQRLIFAGKQLEDGRTLSDYN
AAH08661.1          1 MQIFVKTLTGKTITLEVEPSDTIENVKAKIQDKEGIPPDQQRLIFAGKQLEDGRTLSDYN
PIK45544.1          1 MQIFVKTLTGKTITLEVEPSDTIENVKSKIQDKEGIPPDQQRLIFAGKQLEDGRTLSDYN

TRINITY_DN43805    61 GIPPDQQRLIFPGKQLEDGRTQYQTNIHNETTRQ-PNRYTE------------------
AAA28997.1         61 IQKESTLHLVLRLRGGMQIFVKTLTGKTITLEVEPSDTIENVKAKIQDKEGIPPDQQRLI
AAH08661.1         61 IQKESTLHLVLRLRGGMQIFVKTLTGKTITLEVEPSDTIENVKAKIQDKEGIPPDQQRLI
PIK45544.1         61 IQKESTLHLVLRLRGGMQIFVKTLTGKTITLEVEPSDTIENVKSKIQDKEGIPPDQQRLI

TRINITY_DN43805       ------------------------------------------------------------
AAA28997.1        121 FAGKQLEDGRTLSDYNIQKESTLHLVLRLRGGMQIFVKTLTGKTITLEVEPSDTIENVKA
AAH08661.1        121 FAGKQLEDGRTLSDYNIQKESTLHLVLRLRGGMQIFVKTLTGKTITLDVEPSVTTKKVKQ
PIK45544.1        121 FAGKQLEDGRTLSDYNIQKESTLHLVLRLRGGMQIFVKTLTGKTITLEVEPSDTIENVKS

TRINITY_DN43805       ----------------------------------------------------
AAA28997.1        181 KIQDKEGIPPDQQRLIFAGKQLEDGRTLSDYNIQKESTLHLVLRLRGGIQA
AAH08661.1        181 EDRRTFLTTVSKKSPPCACSWV----------------------------
PIK45544.1        181 KIQDKEGIPQTSSVSSSLVNN-----------------------------
```

D

```
TRINITY_DN16432     1 ----VKTLTGKTITLDVEPSDTIENVKSKIQDKEGIPPDQQSLIFAGKQLEDGRTLSDYN
BAB22630.1          1 MQIFVKTLTGKTITLEVEPSDTIENVKAKIQDKEGIPPDQQRLIFAGKQLEDGRTLSDYN
AAA28997.1          1 MQIFVKTLTGKTITLEVEPSDTIENVKAKIQDKEGIPPDQQRLIFAGKQLEDGRTLSDYN
PIK45544.1          1 MQIFVKTLTGKTITLEVEPSDTIENVKSKIQDKEGIPPDQQRLIFAGKQLEDGRTLSDYN

TRINITY_DN16432    57 IQKESTLHLVLRLRGGMQIFVKTLTGKTITLDVEPSDTIENVKSKIQDKEGIPPDQQSLI
BAB22630.1         61 IQKESTLHLVLRLRGGMQIFVKTLTGKTITLEVEPSDTIENVKAKIQDKEGIPPDQQRLI
AAA28997.1         61 IQKESTLHLVLRLRGGMQIFVKTLTGKTITLEVEPSDTIENVKAKIQDKEGIPPDQQRLI
PIK45544.1         61 IQKESTLHLVLRLRGGMQIFVKTLTGKTITLEVEPSDTIENVKSKIQDKEGIPPDQQRLI

TRINITY_DN16432   117 FAGKQLEDGRTLSDYNIQKESTLHLVLRLRGGMQIFVKTLTGKTITLDVEPSDTIENVKT
BAB22630.1        121 FAGKQLEDGRTLSDYNIQKESTLHLVLRLRGGMQIFVKTLTGKTITLEVEPSDTIENVKA
AAA28997.1        121 FAGKQLEDGRTLSDYNIQKESTLHLVLRLRGGMQIFVKTLTGKTITLEVEPSDTIENVKA
PIK45544.1        121 FAGKQLEDGRTLSDYNIQKESTLHLVLRLRGGMQIFVKTLTGKTITLEVEPSDTIENVKS

TRINITY_DN16432   177 KNQD------------------------------------------------
BAB22630.1        181 KIQDKEGIPPDQQRLIFAGKQLEDGRTLSDYNIQKESTLHLVLRLRGGY--
AAA28997.1        181 KIQDKEGIPPDQQRLIFAGKQLEDGRTLSDYNIQKESTLHLVLRLRGGIQA
PIK45544.1        181 KIQDKEGIPQTSSV--------------SS---------SLVNN-------
```

Preprints (www.preprints.org) | NOT PEER-REVIEWED | Posted: 8 October 2022 doi:10.20944/preprints202210.0087.v1

E

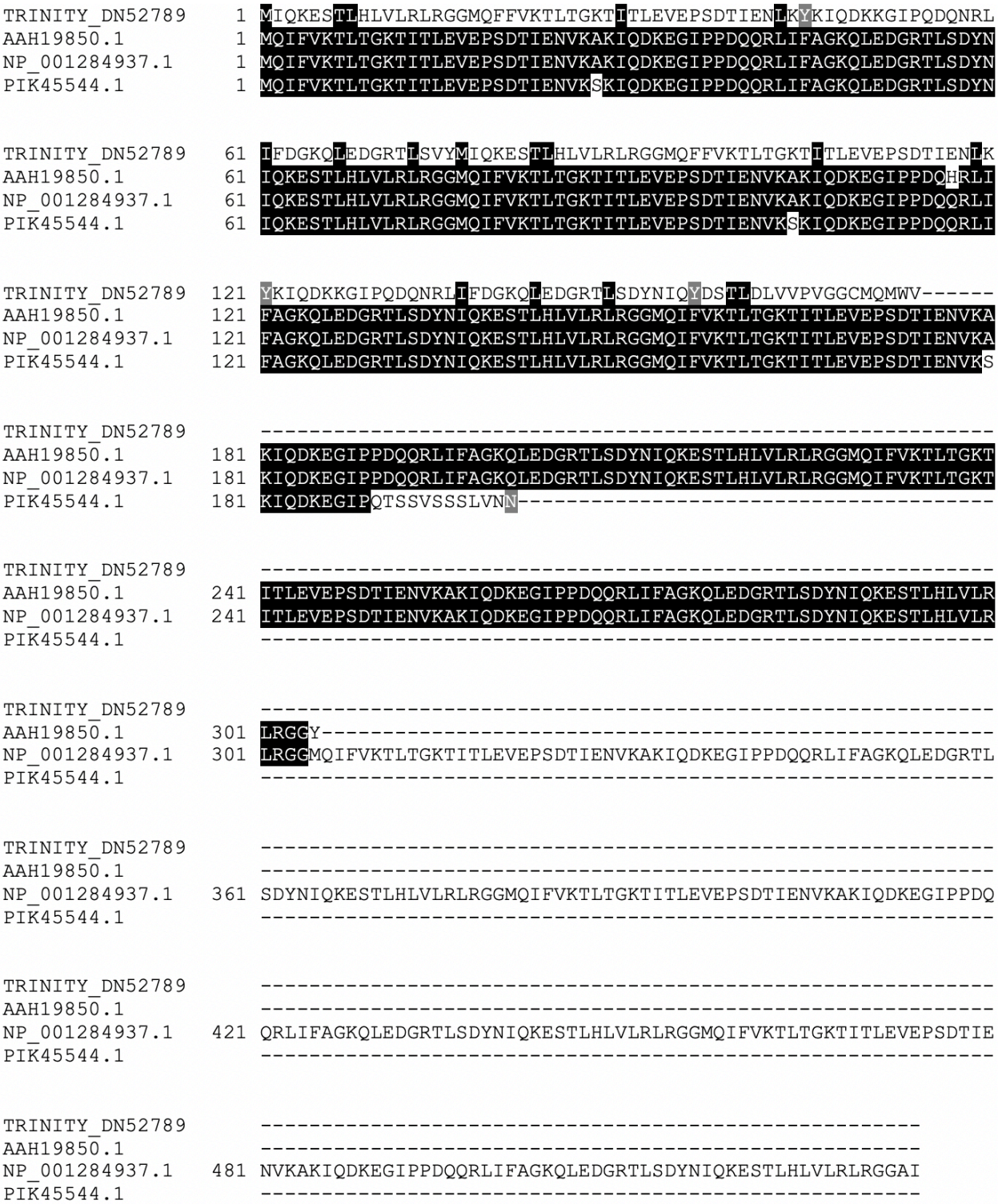

(**B-E**) Alignment of each of the four ubiquitin *H. glaberrima* transcripts with their respective closest matches from the NCBI non-redundant database.

References

1. Mashanov, V.S.; Zueva, O.R.; García-Arrarás, J.E. Transcriptomic Changes during Regeneration of the Central Nervous System in an Echinoderm. *BMC Genomics* **2014**, *15*, 357, doi:10.1186/1471-2164-15-357.
2. Bradbury, E.J.; Burnside, E.R. Moving beyond the Glial Scar for Spinal Cord Repair. *Nat. Commun.* **2019**, *10*, 3879, doi:10.1038/s41467-019-11707-7.

3. Shi, L.-L.; Zhang, N.; Xie, X.-M.; Chen, Y.-J.; Wang, R.; Shen, L.; Zhou, J.-S.; Hu, J.-G.; Lü, H.-Z. Transcriptome Profile of Rat Genes in Injured Spinal Cord at Different Stages by RNA-Sequencing. *BMC Genomics* **2017**, *18*, 173, doi:10.1186/s12864-017-3532-x.
4. Lapuente-Chala, C.; Céspedes-Rubio, A. Biochemical Events Related to Glial Response in Spinal Cord Injury. *Rev. Fac. Med.* **2018**, *66*, 269–277, doi:10.15446/revfacmed.v66n2.61701.
5. Chen, K.; Deng, S.; Lu, H.; Zheng, Y.; Yang, G.; Kim, D.; Cao, Q.; Wu, J.Q. RNA-Seq Characterization of Spinal Cord Injury Transcriptome in Acute/Subacute Phases: A Resource for Understanding the Pathology at the Systems Level. *PLoS ONE* **2013**, *8*, e72567, doi:10.1371/journal.pone.0072567.
6. Li, Y.; Chen, Y.; Li, X.; Wu, J.; Pan, J.-Y.; Cai, R.-X.; Yang, R.-Y.; Wang, X.-D. RNA Sequencing Screening of Differentially Expressed Genes after Spinal Cord Injury. *Neural Regen. Res.* **2019**, *14*, 1583, doi:10.4103/1673-5374.255994.
7. Byrnes, K.R.; Washington, P.M.; Knoblach, S.M.; Hoffman, E.; Faden, A.I. Delayed Inflammatory MRNA and Protein Expression after Spinal Cord Injury. *J. Neuroinflammation* **2011**, *8*, 130, doi:10.1186/1742-2094-8-130.
8. Anthony, D.C.; Couch, Y. The Systemic Response to CNS Injury. *Exp. Neurol.* **2014**, *258*, 105–111, doi:10.1016/j.expneurol.2014.03.013.
9. Sasagawa, S.; Nishimura, Y.; Hayakawa, Y.; Murakami, S.; Ashikawa, Y.; Yuge, M.; Okabe, S.; Kawaguchi, K.; Kawase, R.; Tanaka, T. E2F4 Promotes Neuronal Regeneration and Functional Recovery after Spinal Cord Injury in Zebrafish. *Front. Pharmacol.* **2016**, *7*, doi:10.3389/fphar.2016.00119.
10. Peñailillo, J.; Palacios, M.; Mounieres, C.; Muñoz, R.; Slater, P.G.; De Domenico, E.; Patrushev, I.; Gilchrist, M.; Larraín, J. Analysis of the Early Response to Spinal Cord Injury Identified a Key Role for MTORC1 Signaling in the Activation of Neural Stem Progenitor Cells. *Npj Regen. Med.* **2021**, *6*, 68, doi:10.1038/s41536-021-00179-3.
11. Demircan, T. Dissecting the Molecular Signature of Spinal Cord Regeneration in the Axolotl Model. *Cureus* **2020**, doi:10.7759/cureus.7014.
12. Edwards-Faret, G.; González-Pinto, K.; Cebrián-Silla, A.; Peñailillo, J.; García-Verdugo, J.M.; Larraín, J. Cellular Response to Spinal Cord Injury in Regenerative and Non-Regenerative Stages in *Xenopus laevis*. *Neural Develop.* **2021**, *16*, 2, doi:10.1186/s13064-021-00152-2.
13. Fu, H.; Han, G.; Li, H.; Liang, X.; Hu, D.; Zhang, L.; Tang, P. Identification of Key Genes and Pathways Involved in the Heterogeneity of Intrinsic Growth Ability Between Neurons After Spinal Cord Injury in Adult Zebrafish. *Neurochem. Res.* **2019**, *44*, 2057–2067, doi:10.1007/s11064-019-02841-1.
14. Schmidt-Rhaesa, A.; Harzsch, S.; Purschke, G. *Structure and Evolution of Invertebrate Nervous Systems*; 1st ed.; Oxford University PressOxford, 2015; ISBN 978-0-19-968220-1.
15. Mashanov, V.; Zueva, O. Radial Glia in Echinoderms. *Dev. Neurobiol.* **2018**, dneu.22659, doi:10.1002/dneu.22659.
16. Díaz-Balzac, C.A.; García-Arrarás, J.E. Echinoderm Nervous System. In *Oxford Research Encyclopedia of Neuroscience*; Oxford University Press, 2018 ISBN 978-0-19-026408-6.
17. San Miguel-Ruiz, J.E.; Maldonado-Soto, A.R.; García-Arrarás, J.E. Regeneration of the Radial Nerve Cord in the Sea Cucumber *Holothuria glaberrima*. *BMC Dev. Biol.* **2009**, *9*, 3, doi:10.1186/1471-213X-9-3.
18. Mashanov, V.S.; Zueva, O.R.; García-Arrarás, J.E. Radial Glial Cells Play a Key Role in Echinoderm Neural Regeneration. *BMC Biol.* **2013**, *11*, 49, doi:10.1186/1741-7007-11-49.
19. Mashanov, V.S.; Zueva, O.R.; García-Arrarás, J.E. Myc Regulates Programmed Cell Death and Radial Glia Dedifferentiation after Neural Injury in an Echinoderm. *BMC Dev. Biol.* **2015**, *15*, 24, doi:10.1186/s12861-015-0071-z.
20. Quesada-Díaz, E.; Figueroa-Delgado, P.; García-Rosario, R.; Sirfa, A.; García-Arrarás, J.E. Dedifferentiation of Radial Glia-like Cells Is Observed in in Vitro Explants of Holothurian Radial Nerve Cord. *J. Neurosci. Methods* **2021**, *364*, 109358, doi:10.1016/j.jneumeth.2021.109358.
21. Love, M.I.; Huber, W.; Anders, S. Moderated Estimation of Fold Change and Dispersion for RNA-Seq Data with DESeq2. *Genome Biol.* **2014**, *15*, 550, doi:10.1186/s13059-014-0550-8.
22. Davidson, N.M.; Oshlack, A. Corset: Enabling Differential Gene Expression Analysis for de Novo assembled Transcriptomes. *Genome Biol.* **2014**, *15*, 410, doi:10.1186/s13059-014-0410-6.
23. Camacho, C.; Coulouris, G.; Avagyan, V.; Ma, N.; Papadopoulos, J.; Bealer, K.; Madden, T.L. BLAST+: Architecture and Applications. *BMC Bioinformatics* **2009**, *10*, 421, doi:10.1186/1471-2105-10-421.
24. The UniProt Consortium; Bateman, A.; Martin, M.-J.; Orchard, S.; Magrane, M.; Agivetova, R.; Ahmad, S.; Alpi, E.; Bowler-Barnett, E.H.; Britto, R.; et al. UniProt: The Universal Protein Knowledgebase in 2021. *Nucleic Acids Res.* **2021**, *49*, D480–D489, doi:10.1093/nar/gkaa1100.
25. Tsuboyama, K.; Osaki, T.; Matsuura-Suzuki, E.; Kozuka-Hata, H.; Okada, Y.; Oyama, M.; Ikeuchi, Y.; Iwasaki, S.; Tomari, Y. A Widespread Family of Heat-Resistant Obscure (Hero) Proteins Protect against Protein Instability and Aggregation. *PLOS Biol.* **2020**, *18*, e3000632, doi:10.1371/journal.pbio.3000632.
26. Chen, B.; Piel, W.H.; Gui, L.; Bruford, E.; Monteiro, A. The HSP90 Family of Genes in the Human Genome: Insights into Their Divergence and Evolution. *Genomics* **2005**, *86*, 627–637, doi:10.1016/j.ygeno.2005.08.012.
27. Kabani, M.; Martineau, C. Multiple Hsp70 Isoforms in the Eukaryotic Cytosol: Mere Redundancy or Functional Specificity? *Curr. Genomics* **2008**, *9*, 338–348, doi:10.2174/138920208785133280.
28. Wang, S.; Zheng, Y.; Chen, M.; Storey, K.B. Ultrastructural Variation and Key ER Chaperones Response Induced by Heat Stress in Intestinal Cells of Sea Cucumber *Apostichopus japonicus*. *J. Oceanol. Limnol.* **2021**, *39*, 317–328, doi:10.1007/s00343-020-9265-8.

29. Zhao, H.; Yang, H.; Zhao, H.; Chen, M.; Liu, S. Heat Stress-Mediated Gene Expression in the Body Wall of the Japanese Sea Cucumber *Apostichopus japonicus*. *Aquat. Biol.* **2011**, *12*, 23–31, doi:10.3354/ab00315.
30. Vazzana, M.; Siragusa, T.; Arizza, V.; Buscaino, G.; Celi, M. Cellular Responses and HSP70 Expression during Wound Healing in *Holothuria tubulosa* (Gmelin, 1788). *Fish Shellfish Immunol.* **2015**, *42*, 306–315, doi:10.1016/j.fsi.2014.11.010.
31. Gullian Klanian, M.; Terrats Preciat, M. Effect of PH on Temperature Controlled Degradation of Reactive Oxygen Species, Heat Shock Protein Expression, and Mucosal Immunity in the Sea Cucumber I*sostichopus badionotus*. *PLOS ONE* **2017**, *12*, e0175812, doi:10.1371/journal.pone.0175812.
32. Li, C.; Zhao, W.; Qin, C.; Yu, G.; Ma, Z.; Guo, Y.; Pan, W.; Fu, Z.; Huang, X.; Chen, J. Comparative Transcriptome Analysis Reveals Changes in Gene Expression in Sea Cucumber (*Holothuria leucospilota*) in Response to Acute Temperature Stress. *Comp. Biochem. Physiol. Part D* **2021**, *40*, 100883, doi:10.1016/j.cbd.2021.100883.
33. Patruno, M.; Thorndyke, M.C.; Candia Carnevali, M.D.; Bonasoro, F.; Beesley, P.W. Growth Factors, Heat-Shock Proteins and Regeneration in Echinoderms. *J. Exp. Biol.* **2001**, *204*, 843–848, doi:10.1242/jeb.204.5.843.
34. Parfitt, D.A.; Michael, G.J.; Vermeulen, E.G.M.; Prodromou, N.V.; Webb, T.R.; Gallo, J.-M.; Cheetham, M.E.; Nicoll, W.S.; Blatch, G.L.; Chapple, J.P. The Ataxia Protein Sacsin Is a Functional Co-Chaperone That Protects against Polyglutamine-Expanded Ataxin-1. *Hum. Mol. Genet.* **2009**, *18*, 1556–1565, doi:10.1093/hmg/ddp067.
35. Al-Ramahi, I.; Lam, Y.C.; Chen, H.-K.; de Gouyon, B.; Zhang, M.; Pérez, A.M.; Branco, J.; de Haro, M.; Patterson, C.; Zoghbi, H.Y.; et al. CHIP Protects from the Neurotoxicity of Expanded and Wild-Type Ataxin-1 and Promotes Their Ubiquitination and Degradation. *J. Biol. Chem.* **2006**, *281*, 26714–26724, doi:10.1074/jbc.M601603200.
36. Park, B.-J.; Lee, D.-G.; Yu, J.-R.; Jung, S.; Choi, K.; Lee, J.; Lee, J.; Kim, Y.S.; Lee, J.I.; Kwon, J.Y.; et al. Calreticulin, a Calcium-Binding Molecular Chaperone, Is Required for Stress Response and Fertility in *Caenorhabditis Elegans*. *Mol. Biol. Cell* **2001**, *12*, 2835–2845, doi:10.1091/mbc.12.9.2835.
37. Davis, C.O.; Kim, K.-Y.; Bushong, E.A.; Mills, E.A.; Boassa, D.; Shih, T.; Kinebuchi, M.; Phan, S.; Zhou, Y.; Bihlmeyer, N.A.; et al. Transcellular Degradation of Axonal Mitochondria. *Proc. Natl. Acad. Sci.* **2014**, *111*, 9633–9638, doi:10.1073/pnas.1404651111.
38. Hayakawa, K.; Esposito, E.; Wang, X.; Terasaki, Y.; Liu, Y.; Xing, C.; Ji, X.; Lo, E.H. Transfer of Mitochondria from Astrocytes to Neurons after Stroke. *Nature* **2016**, *535*, 551–555, doi:10.1038/nature18928.
39. Miller, D.J.; Fort, P.E. Heat Shock Proteins Regulatory Role in Neurodevelopment. *Front. Neurosci.* **2018**, *12*, 821, doi:10.3389/fnins.2018.00821.
40. Turturici, G.; Sconzo, G.; Geraci, F. Hsp70 and Its Molecular Role in Nervous System Diseases. *Biochem. Res. Int.* **2011**, *2011*, 1–18, doi:10.1155/2011/618127.
41. Brown, I.R. Heat Shock Proteins and Protection of the Nervous System. *Ann. N. Y. Acad. Sci.* **2007**, *1113*, 147–158, doi:10.1196/annals.1391.032.
42. Latchman, D. Protective Effect of Heat Shock Proteins in the Nervous System. *Curr. Neurovasc. Res.* **2004**, *1*, 21–27, doi:10.2174/1567202043480206.
43. Shang, F.; Taylor, A. Ubiquitin–Proteasome Pathway and Cellular Responses to Oxidative Stress. *Free Radic. Biol. Med.* **2011**, *51*, 5–16, doi:10.1016/j.freeradbiomed.2011.03.031.
44. Patruno, M.; Thorndyke, M.C.; Candia Carnevali, M.D.; Bonasoro, F.; Beesley, P. Changes in Ubiquitin Conjugates and Hsp72 Levels During Arm Regeneration in Echinoderms. *Mar. Biotechnol.* **2001**, *3*, 4–15, doi:10.1007/s101260000018.
45. Pasten, C.; Ortiz-Pineda, P.A.; García-Arrarás, J.E. Ubiquitin-Proteasome System Components Are Upregulated during Intestinal Regeneration. *genesis* **2012**, *50*, 350–365, doi:10.1002/dvg.20803.
46. Pasten, C.; Rosa, R.; Ortiz, S.; González, S.; García-Arrarás, J.E. Characterization of Proteolytic Activities during Intestinal Regeneration of the Sea Cucumber, *Holothuria glaberrima*. *Int. J. Dev. Biol.* **2012**, *56*, 681–691, doi:10.1387/ijdb.113473cp.
47. Dubois, M.-L.; Meller, A.; Samandi, S.; Brunelle, M.; Frion, J.; Brunet, M.A.; Toupin, A.; Beaudoin, M.C.; Jacques, J.-F.; Lévesque, D.; et al. UBB Pseudogene 4 Encodes Functional Ubiquitin Variants. *Nat. Commun.* **2020**, *11*, 1306, doi:10.1038/s41467-020-15090-6.
48. Imai, Y.; Soda, M.; Hatakeyama, S.; Akagi, T.; Hashikawa, T.; Nakayama, K.-I.; Takahashi, R. CHIP Is Associated with Parkin, a Gene Responsible for Familial Parkinson's Disease, and Enhances Its Ubiquitin Ligase Activity. *Mol. Cell* **2002**, *10*, 55–67, doi:10.1016/S1097-2765(02)00583-X.
49. Joshi, V.; Amanullah, A.; Upadhyay, A.; Mishra, R.; Kumar, A.; Mishra, A. A Decade of Boon or Burden: What Has the CHIP Ever Done for Cellular Protein Quality Control Mechanism Implicated in Neurodegeneration and Aging? *Front. Mol. Neurosci.* **2016**, *9*, doi:10.3389/fnmol.2016.00093.
50. Muchowski, P.J.; Wacker, J.L. Modulation of Neurodegeneration by Molecular Chaperones. *Nat. Rev. Neurosci.* **2005**, *6*, 11–22, doi:10.1038/nrn1587.
51. Tabas, I.; Ron, D. Integrating the Mechanisms of Apoptosis Induced by Endoplasmic Reticulum Stress. *Nat. Cell Biol.* **2011**, *13*, 184–190, doi:10.1038/ncb0311-184.
52. Pramanik, J.; Chen, X.; Kar, G.; Henriksson, J.; Gomes, T.; Park, J.-E.; Natarajan, K.; Meyer, K.B.; Miao, Z.; McKenzie, A.N.J.; et al. Genome-Wide Analyses Reveal the IRE1a-XBP1 Pathway Promotes T Helper Cell Differentiation by Resolving Secretory Stress and Accelerating Proliferation. *Genome Med.* **2018**, *10*, 76, doi:10.1186/s13073-018-0589-3.
53. Casas-Tinto, S.; Zhang, Y.; Sanchez-Garcia, J.; Gomez-Velazquez, M.; Rincon-Limas, D.E.; Fernandez-Funez, P. The ER Stress Factor XBP1s Prevents Amyloid-β Neurotoxicity. *Hum. Mol. Genet.* **2011**, *20*, 2144–2160, doi:10.1093/hmg/ddr100.

54. Sinzelle, L.; Carradec, Q.; Paillard, E.; Bronchain, O.J.; Pollet, N. Characterization of a *Xenopus Tropicalis* Endogenous Retrovirus with Developmental and Stress-Dependent Expression. *J. Virol.* **2011**, *85*, 2167–2179, doi:10.1128/JVI.01979-10.
55. Mashanov, V.S.; Zueva, O.R.; García-Arrarás, J.E. Posttraumatic Regeneration Involves Differential Expression of Long Terminal Repeat (LTR) Retrotransposons. *Dev. Dyn.* **2012**, *241*, 1625–1636, doi:10.1002/dvdy.23844.
56. Pakos-Zebrucka, K.; Koryga, I.; Mnich, K.; Ljujic, M.; Samali, A.; Gorman, A.M. The Integrated Stress Response. *EMBO Rep.* **2016**, *17*, 1374–1395, doi:10.15252/embr.201642195.
57. Taniuchi, S.; Miyake, M.; Tsugawa, K.; Oyadomari, M.; Oyadomari, S. Integrated Stress Response of Vertebrates Is Regulated by Four EIF2α Kinases. *Sci. Rep.* **2016**, *6*, 32886, doi:10.1038/srep32886.
58. Hai, T.; Curran, T. Cross-Family Dimerization of Transcription Factors Fos/Jun and ATF/CREB Alters DNA Binding Specificity. *Proc. Natl. Acad. Sci.* **1991**, *88*, 3720–3724, doi:10.1073/pnas.88.9.3720.
59. Bhoumik, A.; Takahashi, S.; Breitweiser, W.; Shiloh, Y.; Jones, N.; Ronai, Z. ATM-Dependent Phosphorylation of ATF2 Is Required for the DNA Damage Response. *Mol. Cell* **2005**, *18*, 577–587, doi:10.1016/j.molcel.2005.04.015.
60. Mangelsdorf, D.J.; Evans, R.M. The RXR Heterodimers and Orphan Receptors. *Cell* **1995**, *83*, 841–850, doi:10.1016/0092-8674(95)90200-7.
61. Cao, X.; Liu, W.; Lin, F.; Li, H.; Kolluri, S.K.; Lin, B.; Han, Y.; Dawson, M.I.; Zhang, X. Retinoid X Receptor Regulates Nur77/Thyroid Hormone Receptor 3-Dependent Apoptosis by Modulating Its Nuclear Export and Mitochondrial Targeting. *Mol. Cell. Biol.* **2004**, *24*, 9705–9725, doi:10.1128/MCB.24.22.9705-9725.2004.
62. Quispe-Parra, D.J.; Medina-Feliciano, J.G.; Cruz-González, S.; Ortiz-Zuazaga, H.; García-Arrarás, J.E. Transcriptomic Analysis of Early Stages of Intestinal Regeneration in *Holothuria glaberrima*. *Sci. Rep.* **2021**, *11*, 346, doi:10.1038/s41598-020-79436-2.
63. Sherman, B.T.; Hao, M.; Qiu, J.; Jiao, X.; Baseler, M.W.; Lane, H.C.; Imamichi, T.; Chang, W. DAVID: A Web Server for Functional Enrichment Analysis and Functional Annotation of Gene Lists (2021 Update). *Nucleic Acids Res.* **2022**, *50*, W216–W221, doi:10.1093/nar/gkac194.
64. Supek, F.; Bošnjak, M.; Škunca, N.; Šmuc, T. REVIGO Summarizes and Visualizes Long Lists of Gene Ontology Terms. *PLoS ONE* **2011**, *6*, e21800, doi:10.1371/journal.pone.0021800.
65. Bello, S.A.; Torres-Gutiérrez, V.; Rodríguez-Flores, E.J.; Toledo-Román, E.J.; Rodríguez, N.; Díaz-Díaz, L.M.; Vázquez-Figueroa, L.D.; Cuesta, J.M.; Grillo-Alvarado, V.; Amador, A.; et al. Insights into Intestinal Regeneration Signaling Mechanisms. *Dev. Biol.* **2020**, *458*, 12–31, doi:10.1016/j.ydbio.2019.10.005.